

Pores of No Return

David W. Andrews^{1,*}

¹Sunnybrook Research Institute and Department of Biochemistry, University of Toronto, Toronto, ON M4N 3M5, Canada

*Correspondence: david.andrews@sri.utoronto.ca

<http://dx.doi.org/10.1016/j.molcel.2014.11.005>

In this issue, [Bleicken et al. \(2014\)](#) use double electron-electron resonance (DEER) spectroscopy to propose a new model for the active form of Bax at membranes that differs significantly from those previously proposed.

During programmed cell death, mitochondrial membrane permeabilization is often the tightly regulated point of no return. During this process, cellular responses to stress are interpreted by a complex interplay between pro- and anti-apoptotic Bcl-2 family proteins that determines whether the outer-mitochondrial membrane will be permeabilized by the proapoptotic executor proteins Bax and Bak ([Chi et al., 2014](#)). Despite more than 25 years of intense investigation, the molecular mechanisms by which these and other helical pore-forming proteins penetrate and permeabilize membranes remain mysterious, partly due to the difficulty in determining the structures of membrane protein complexes. For Bax, structure determination has been made more difficult by the large size of the holes made in membranes. However, by measuring the active form of Bax at membranes, [Bleicken et al. \(2014\)](#) now propose a provocative new 3D model of the membrane-bound protein that is very different than its predecessors.

To construct this model, [Bleicken et al. \(2014\)](#) used a form of electron paramagnetic resonance spectroscopy called double electron-electron resonance (DEER) spectroscopy. This technique allows precise measurements of the distance between a pair of probes attached to cysteine residues. By making mutants with one or two cysteine residues at defined locations, they measured distances within and between active Bax proteins incubated with liposomes. These measurements serve as a series of constraints that can be used to iteratively build and test a model of a membrane protein or complex. However, the process is greatly facilitated by using a model as a starting point.

A number of models for the structure of the membrane-permeabilizing form of

Bax have been published. Most are based on the similarity in the overall fold of the solution form of Bax to that of other α -helical pore-forming proteins such as diphtheria toxin. In conventional models for the pore-forming form of Bax, 1–4 (most frequently 3) of the Bax α helices span the membrane, similar to the transmembrane sequences found in many proteins ([Figure 1A](#)). This seemed a logical assumption based on the length and hydrophobicity of several of the helices in Bax. However, the only helix sufficiently hydrophobic to be entirely buried in the bilayer is helix 9. Chemical labeling and fluorescence spectroscopy experiments suggested that hydrophobic residues in helices 5, 6, and 9 are likely to be exposed to the lipid core of membranes, although some residues in helices 5 and 6 remained accessible to the aqueous milieu ([Annis et al., 2005](#); [Lovell et al., 2008](#)). Thus, it was commonly proposed that helices 5 and 6 line a lipidic pore with the hydrophobic residues embedded in the bilayer, the head groups of the lipids nestled between the helices and aqueous exposed residues lining the water-filled cavity. However, these models are difficult to reconcile with observations suggesting that the BH3 binding region of Bax remains intact and accessible to BH3-protein binding even after Bax has inserted into the membrane.

Inconsistencies between recent crystallography data prompted a rethinking of and reanalysis of conventional pore models ([Czabotar et al., 2013](#); [Westphal et al., 2014](#)). Critically important was the observation that the core substructure was unlikely to unfold to generate multiple conventional transmembrane helices. Furthermore, for Bak it was possible to attach this core complex to the bilayer in such a way that side chains protected from chemical labeling by interaction

with the membrane could embed in the lipids without helices 5 and 6 crossing the bilayer. The result was a pore-complex model ([Figure 1B](#)) in which only helix 9 embeds into the lipid bilayer, with the rest of the protein engaged as a dimer bound to the membrane surface with helices 5 and 6 partially inserted in the membrane ([Czabotar et al., 2013](#); [Westphal et al., 2014](#)). These models propose a further conformational change to partially insert helices 6 and 7 into the membrane but do not fully explain how Bax molecules with a single transmembrane region (helix 9) form a stable pore.

Using the crystal structure of the core complex of Bax as a starting point, [Bleicken et al. \(2014\)](#) introduced cysteine residues at defined locations within Bax and measured the distance between them using DEER. The correspondence between the DEER and the crystallography data confirm that the complex core structure of the Bax dimer is present in the active membrane-bound form of Bax. Surprisingly, several distance measurements were inconsistent with all of the previous models; the new model developed by the authors therefore has a number of intriguing characteristics. The most remarkable feature is that the membrane-embedded Bax dimer is comprised of monomers in opposite orientations on/in the membrane. Thus, the dimeric core domain lines a lipidic pore with the strongly amphipathic helix 6 of each monomer lying on the surface of opposite leaflets ([Figure 1B](#), top). These partially embedded helices tether helices 7–9 to the core domain but allow them to extend about 2 nm away from it. The DEER data strongly suggest that these helices are mobile within and on the bilayer. In retrospect, this result may explain why previously published fluorescence spectroscopy, chemical labeling,

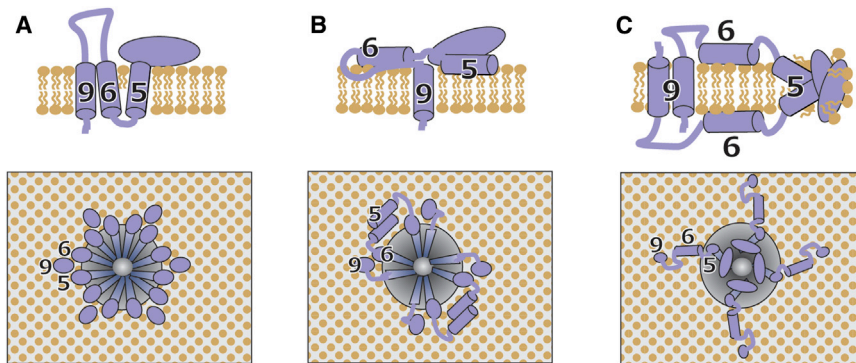


Figure 1. Bax Lipidic Pore Models

(A–C) For all models, the number of monomers is arbitrary. The monomer (A and B) or dimer (C) is shown from the side in each top panel. The oligomer is shown from the top in each lower panel. Cylinders denote the helices, and the oval represents the amino-terminal domain.

(A) Bax inserts helix 9 into the bilayer, followed by a structural rearrangement driven by membrane binding and dimerization that results in helices 5 and 6 inserting in a transmembrane orientation and interacting with helix 9. Together, all three helices stabilize the pore. The amphipathic nature of helices 5 and 6, and interfaces in the amino terminus, drive oligomerization of dimers to form a pore.

(B) Bax unlatches to form a dimer that binds membranes with helix 9 embedded across the bilayer and helices 5 and 6 spread on the surface of the membrane with their hydrophobic residues inserted into the bilayer. Oligomerization involves an interface between helix 2 and potentially other regions of each monomer. A conformational change subsequent to oligomer formation inserts helices 7–9 to line/stabilize the pore.

(C) Bax dimers penetrate and wrap around and through the bilayer such that the two monomers occupy opposite faces of the membrane. The dimer core interacts with lipids via the hydrophobic faces of helices 5 and 6. Subsequent to or coincident with oligomerization, interactions between the hydrophilic parts of the dimer core drive formation of a lipidic pore lined by core-domain dimers tethered to transmembrane helix 9 anchors by amphipathic helix 6 regions bound to the membrane surfaces by hydrophobic residues that insert into the bilayer. In the top view, the second monomers on the opposite side of the membrane for each dimer are not shown.

and crosslinking data often suggested intermediate phenotypes (Annis et al., 2005; Lovell et al., 2008; Zhang et al., 2010; Westphal et al., 2014). The model suggests that helix 9 acts like an anchor in the bilayer by interacting with the helix 9 from the other monomer in the dimer that is in the opposite orientation in the membrane. This results in an anchor that spans the membrane from both sides with tethers in each leaflet (Figure 1C). Unlike models in which a lipid pore is held open by a single Bax monomer (Volkman et al., 2014), this is a very attractive configuration for maintaining the structure of a constitutively open pore structure (Figure 1B, lower). The mobility of the membrane-embedded region may also facilitate the oligomerization of membrane-bound dimers required to form a pore.

As attractive as the final model of Bleicken et al. (2014) is, the path between

soluble monomers and membrane-embedded dimers is unclear. Unlike the conventional models (Figures 1A and 1B) where individual helices can slip into the bilayer, for the new model (Figure 1C) it is very difficult to envision how one monomer of the dimer transits across to the opposite face of the bilayer to insert in the other leaflet (Figure 1C, top). In the absence of a pore, as would be the case when Bax first inserts into the membrane, the thermodynamic cost of embedding the relatively hydrophilic dimerized core domain into bilayer must be very high. Whether dimerization on the membrane provides sufficient energy to destabilize the lipids sufficiently to provoke their rearrangement into a lipidic pore and to drive one monomer across the bilayer remains to be determined. The high energy barrier may explain why Bax insertion into the membrane rather than oligomerization is rate-limiting (Lovell

et al., 2008). Furthermore, the instability that results from embedding the dimeric core domain of membrane-bound Bax may drive oligomerization.

Another unknown is the number of dimers that must oligomerize to permeabilize the membrane to large proteins. Estimates for the number of Bax monomers in a pore vary from one to thousands (Volkman et al., 2014; Satsoura et al., 2012). The provocative new model proposed by Bleicken et al. (2014) does not predict the number of Bax required to permeabilize a membrane but will undoubtedly fuel many conversations and productive future avenues of research.

ACKNOWLEDGMENTS

Research in the author's laboratory is funded by grant FRN 12517 from the Canadian Institutes Health Research.

REFERENCES

- Annis, M.G., Soucie, E.L., Dlugosz, P.J., Cruz-Aguado, J.A., Penn, L.Z., Leber, B., and Andrews, D.W. (2005). *EMBO J.* 24, 2096–2103.
- Bleicken, S., Jeschke, G., Stegmüller, C., Salvador-Gallego, R., García-Sáez, A.J., and Bordignon, E. (2014). *Mol. Cell* 56, this issue, 496–505.
- Chi, X., Kale, J., Leber, B., and Andrews, D.W. (2014). *Biochim. Biophys. Acta* 1843, 2100–2113.
- Czabotar, P.E., Westphal, D., Dewson, G., Ma, S., Hockings, C., Fairlie, W.D., Lee, E.F., Yao, S., Robin, A.Y., Smith, B.J., et al. (2013). *Cell* 152, 519–531.
- Lovell, J.F., Billen, L.P., Bindner, S., Shamas-Din, A., Fradin, C., Leber, B., and Andrews, D.W. (2008). *Cell* 135, 1074–1084.
- Satsoura, D., Kučerka, N., Shivakumar, S., Pencser, J., Griffiths, C., Leber, B., Andrews, D.W., Katsaras, J., and Fradin, C. (2012). *Biochim. Biophys. Acta* 1818, 384–401.
- Volkman, N., Marassi, F.M., Newmeyer, D.D., and Hanein, D. (2014). *Cell Death Differ.* 21, 206–215.
- Westphal, D., Dewson, G., Menard, M., Frederick, P., Iyer, S., Bartolo, R., Gibson, L., Czabotar, P.E., Smith, B.J., Adams, J.M., and Kluck, R.M. (2014). *Proc. Natl. Acad. Sci. USA* 111, E4076–E4085.
- Zhang, Z., Zhu, W., Lapolla, S.M., Miao, Y., Shao, Y., Falcone, M., Boreham, D., McFarlane, N., Ding, J., Johnson, A.E., et al. (2010). *J. Biol. Chem.* 285, 17614–17627.